

Relationship between the Structure of C_{60} and its Lubricity: a Review

Abstract

Based on analyses of the calculations of quantum theories, such as electron charge density, the energy level distribution of orbitals, and the forces between C atoms and between the molecules in C_{60} crystals, the author concludes that C_{60} crystal is a promising solid lubricant. Furthermore, owing to the unique spherical structure of its molecules, high chemical stability, and the phase transition of the crystal fullerene C_{60} may have some particular tribological properties that are superior to traditional graphite and MoS_2 , especially under crucial conditions such as high vacuum, high pressure or in a humid environment. The tribological tests that have been reported show the lubricity of fullerene C_{60} , and the effects of the lubricating properties of C_{60} on some metals are also predicted.

Keywords

fullerene, C_{60} , structure, lubricity, electron charge density, molecules

INTRODUCTION

It is well known that there are two kinds of pure carbon, i.e. graphite and diamond. Diamond is a modified face-centred cubic (FCC) lattice. Each of its carbon atoms is bonded to four others by sp^3 hybridised orbitals, which forms a tetrahedral structure. Graphite is a layered crystal with a hexagonal-closed packed (HCP) lattice. The carbon atoms in each layer of graphite are bonded by sp^2 hybridised orbitals, and the adjacent layers combined by weak van der Waals forces. These layers can slide easily over one another; graphite is thus widely used as a solid lubricant.

However, in recent years, a third form of pure carbon – carbon clusters or so called ‘fullerenes’ – has been found. In early 1990, Kratschmer *et al.*¹ reported the preparation of fullerene C_{60} and C_{70} in bulk quantities. This discovery has interested researchers in many different disciplines, and a number of valuable facts about these materials have already been obtained. Unlike graphite and diamond, which are infinite

Figure 1 Sketch of fullerene C_{60} structure. The dashed line relates to Figure 4

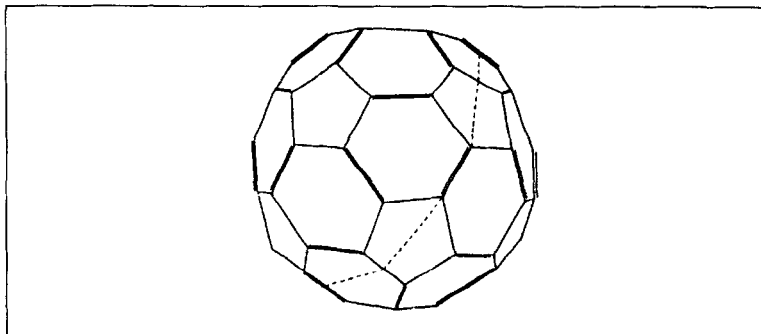


Table 1 Physical properties of fullerene C_{60}

<i>Property</i>	<i>Description</i>
Colour	Black (powder)
Structure of crystal	FCC lattice (Fm3m) at room temp. $a = 14.17\text{-}14.20\text{\AA}$ SC lattice (Pa3) below $249\text{-}260^\circ\text{K}$ $a = 14.06\text{-}14.078\text{\AA}$ [2-6]
Sublimation temp.	$673\text{-}723^\circ\text{K}$ (stable in air)
Density	$1.68\text{-}1.70\text{ g/cm}^3$ (FCC)
Dissolving solvents	Wide range of non-polar solvents, e.g., benzene, toluene, hexane, CS_2
Bulk modulus	18 GPa (FCC)
Refractive index	2.2 at 630 nm wavelength
Heat of formation	$415\text{-}490\text{ Kcal/mol}$, 582 Kcal/mol , 14.5 Kcal/mol per C atom RHF [7] STO-3G [7, 8] MNDO [9]

periodic network solids, the fullerene is a molecular form of pure carbon, and is finite. All members of this new molecular class share one property in common: they are hollow, geodesic spheroids, as shown in **Figure 1**. The spherical shells are networks of pentagons and hexagons with covalently bonded carbon atoms. Any such network must have 12 pentagons, although the members of the hexagons can vary widely. Fullerene molecules may have carbon numbers ranging from 32 to 960. However, the most stable molecule is C_{60} , then C_{70} . Fullerene C_{60} , with 12 pentagons and 20 hexagons, has the most stable spherical structure.

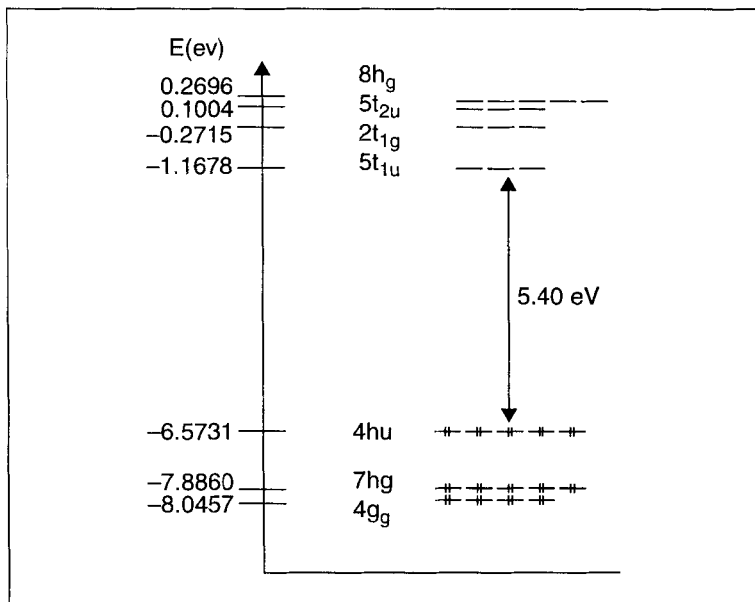
In a C_{60} molecule, each carbon atom is bonded to three adjacent carbon atoms by σ covalent bonds of $\text{sp}^{2.278}$ hybridised orbitals, and 60 carbon atoms form a delocalised π bond over the geodesic spheroid.

Table 2 Structural properties of fullerene C₆₀

<i>Property</i>	<i>Description</i>
Structure of C ₆₀ molecule	Spherical cage with 12 pentagons and 20 hexagons, diameter of 7.1 Å, symmetry of Ih
Interatomic bond	Each carbon atom bonded to three adjacent carbon atoms by sp ^{2.278} hybridised σ-orbitals 60 carbon atoms forming a delocalised π bond over the geodesic spheroid by s ^{0.093} p hybridised orbitals POAV ^{10,11}
Bond length:	
Carbon atoms shared by:	
– two hexagons	6:6 C-C 1.36-1.41 Å
– a hexagon	6:5 C-C 1.43-1.47 Å
– and a pentagon	MNDO, ⁹ INDO, ^{12,13} CNDO/S, ¹⁴ POAV, ¹⁵ PPPCI, ¹⁶ LMTO, ¹⁷ STO-3G, ^{8,18} QCFF/PI, ¹⁹ GGA, ²⁰ LDA ²¹
Bond angle	θσ-σ=116° (bond angle of 120° in planar sp ²) θσ-π=101.6° (11.6° deviated from planar sp ²) POAV ^{10,15}
Bond order	6:6 C-C 0.54-0.60 MNDO, ⁹ POAV 6:5 C-C 0.41-0.476, ¹⁵ LMTO ¹⁷
Bond energy	7.24-8.50 eV/atom (calculation) 6.94-6.98 eV/atom (experiment) GGA, ²⁰ LDA ^{20,21}
Resonance energy	0.533 β/C atom (relative to 0.333 β/C atom in the benzene and 0.576 β/C atom in graphite, ethylene based). ^{10,15,22}
Interaction between C ₆₀ molecules (cohesive energy)	1.5-1.99 eV/C ₆₀ ^{3,23-25}
Distance between adjacent molecules	10.02 ± 0.01 Å ^{24,26}
HOMO-LUMO gap	1.04-2.15 eV, 3.75 eV (calculation) 1.85-2.70 eV (experiment) GGA, ²⁰ LSD, ²⁷ LDA, ^{21,28} QP, ²⁸ NWC, ²⁹ PES/IPES ^{3,30,31}
Electron affinity	0.8 eV, 2.4-2.8 eV (calculation) 2.65-2.80 eV (experiment) CNDO/S, ¹⁴ LSD, ²⁷ PO ²⁷
Ionisation energy	7.4-8.5 eV (calculation) 6.42-7.87 eV (experiment) STO-3G, ^{8,18} LSD, ²⁷ MNDO, ³² DV, ³³ XRD, ⁴ XPS, UPS ³⁴

Thus, the C₆₀ molecule is a geodesic cage or a geodesic dome with 32 polygons, and also called a 'soccer-molecule'. Fullerene C₆₀ is soft, because of the weak van der Waals forces between its molecules, and is easily compressed. Miller²

Figure 2 Molecular-orbital energy level diagram for C₆₀ from INDO



predicted that solid C₆₀ could be used as a solid lubricant, with the spherical C₆₀ molecules acting as tiny ball bearings.

The present paper analyses quantum research on the structure of C₆₀, and discusses the relation between the C₆₀ structure and its lubricity, and also looks at the results of some tribological tests that have been reported.

THEORY OF C₆₀ STRUCTURE

The physical properties of fullerene C₆₀ are shown in **Table 1**.

Data on the theoretical investigations into the structure of the C₆₀ molecule and crystal are summarised in **Table 2**. For comparison, some experimental data are also given.

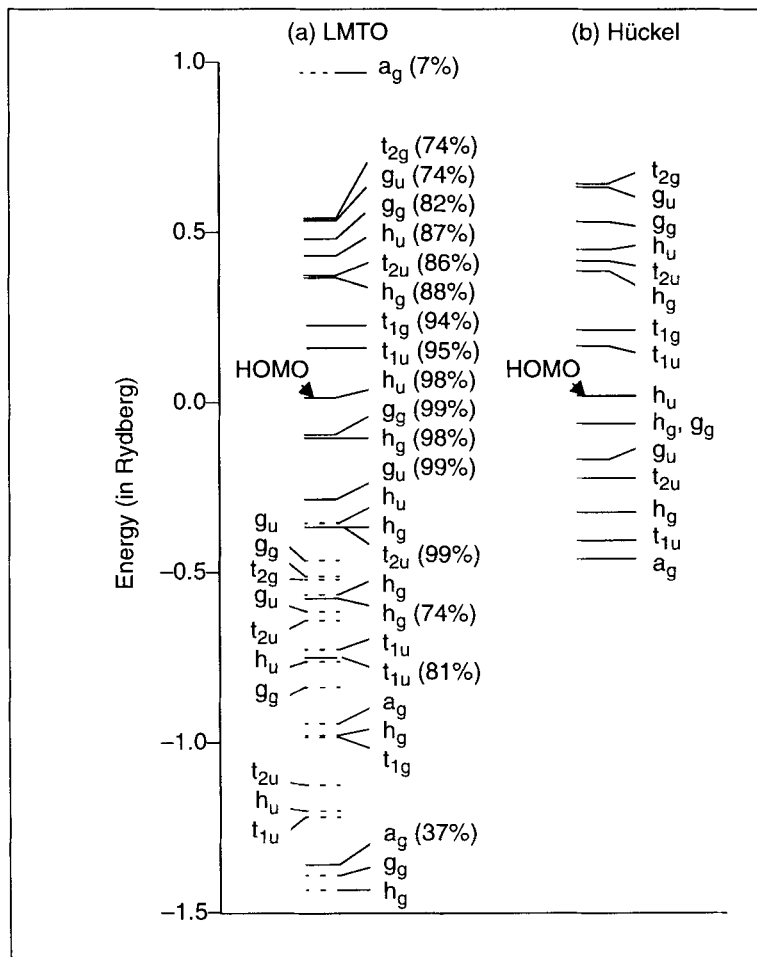
Figures 2¹² and **3**¹⁷ are given as examples of energy level diagrams for the C₆₀ molecule. These diagrams are based on INDO, LMTO and Huckel calculations.

The distribution of electronic charges is illustrated in **Figures 4**¹⁷ (see overleaf) and **5** (see p.187).³⁵

DISCUSSION

Although the data from the different calculations are not all the same, they have a semi-quantitative or qualitative consistency, and are in good agreement with experiments.

Figure 3 Molecular-orbital scheme with orbital symmetries as obtained from the *ab initio* LMT0 calculation (a). In parentheses are the carbon p_z orbital values of the MOs with predominant C-p_z contribution. (b) The results of a Hückel calculation with one orbital per atom and nearest-neighbour hopping integral $\beta = 0.20$ Ryd (1 hartree = 2 rydberg = 27.2 eV)



The curvature of the fullerene C₆₀ molecular surface makes its orbitals different from those of planar graphite or benzene. As the π bonds at conjugated carbon atoms deviate from planarity, σ and p_z orbitals rehybridise so that a π -orbital is no longer a purely p-orbital component, and the σ orbitals no longer contain all the s-orbital component. The σ -orbitals have sp^{2.278} hybridisation, which inclines toward the intramolecule at 11.6°. The delocalised 8^{0.093}p π -bond is distributed over the geodesic spheroid. Thus, fullerene C₆₀ is of intermediate hybridisation. The angle between the σ and π -orbitals ($\theta_{\sigma-\pi}$) is

Figure 4 Contours showing valence-electron density on a plane passing through the centre of the cluster and two 6-6 bonds. (a) The intersection of this plane with the spherical shell of carbon atoms is indicated by the dashed line in Figure 1. The plane contains four carbon atoms and passes through the mid-points of six other C-C bonds. The values for the electron density are in units of 10^{-2} e/au^3 . (b) The valence-electron densities along two radial directions (indicated by *ab* and *ac* in (a)) as a function of distance *d* from the centre of the cluster. Also shown here is the total number of electrons enclosed by the sphere of radius *d* located at the centre of the cluster. *r₀* on the x axis indicates the position of carbon atoms.

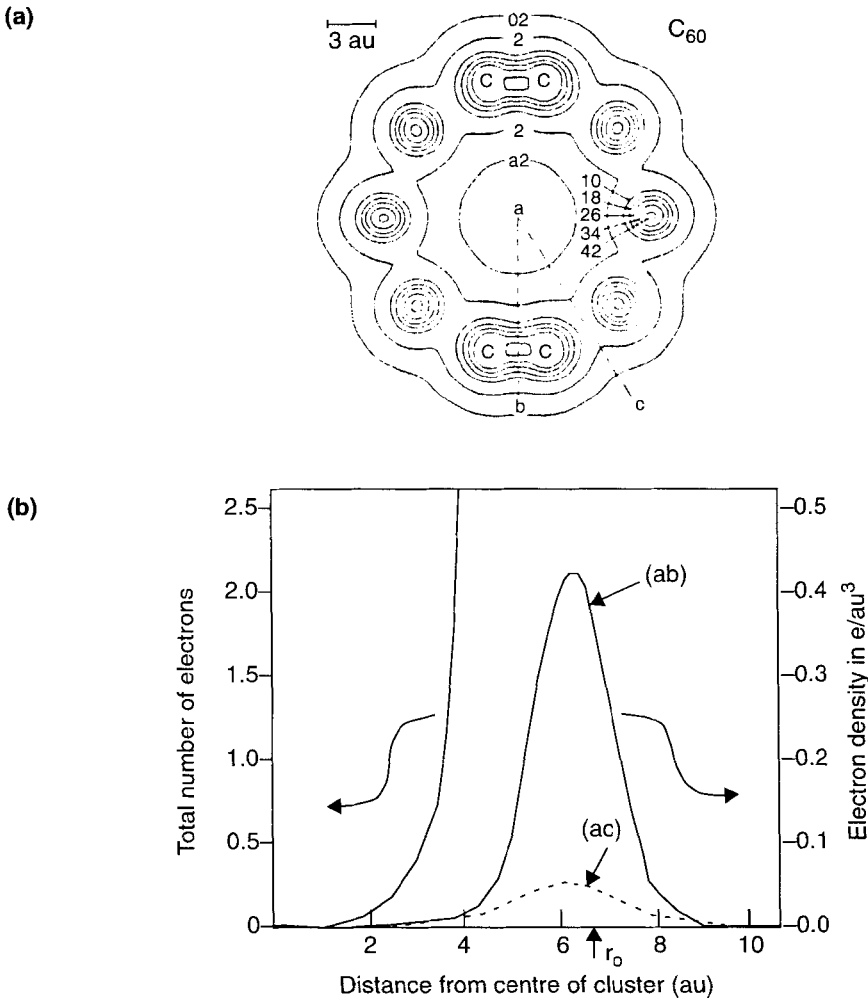
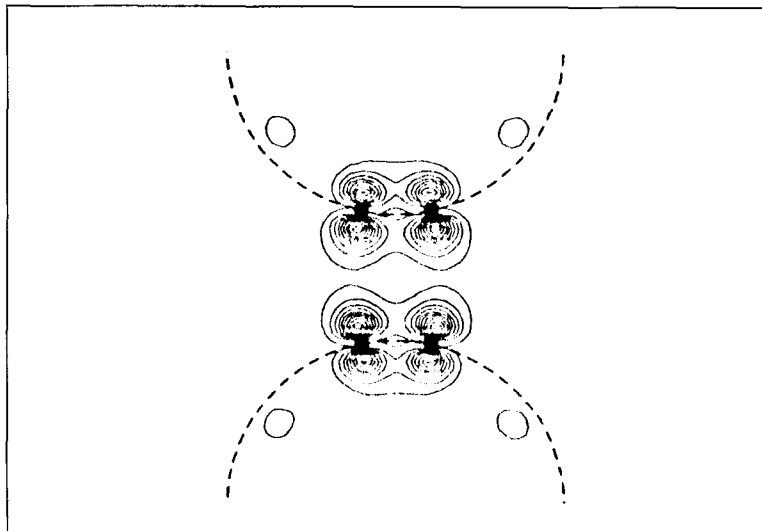


Figure 5 Calculated charge density distribution of t_{1u} LUMO electrons, shown in a plane (close to (110)) containing two pairs of atoms on adjacent molecules



not the usual 90° , but 101.6° . 240 valent electrons fill up to the highest-occupied fivefold degenerate h_u (HOMO) level. Molecular orbitals with a predominant p_z component dominate the molecular orbital scheme around the Fermi energy, i.e. the energy of the HOMO.

Each carbon atom in C_{60} molecules is on the vertexes shared by a pentagon and two hexagons, and forms two kinds of bonds, usually shown as 6:6 C-C and 6:5 C-C. The group-theoretic analysis of the molecular orbitals in itself indicates that the 6:6 C-C bond should have a larger bond order than the 6:5 C-C bond, and should be the stronger. From the calculations, the 6:6 C-C bond (usually called the 'double bond') is shorter than the 6:5 C-C bond (the 'single bond'). This is similar to the conjugated systems in benzene and butadiene.

The covalent bonds between carbon atoms within a fullerene C_{60} molecule are very strong (bond energy of 6.94-8.50 eV/C atom). The molecules themselves bond together only weakly through van der Waals forces (cohesive energy of 1.50-1.99 eV/ C_{60}). That is, solid C_{60} is a molecular crystal. If the molecular interaction is only regarded as Coulomb interaction (U), the on-site molecular C_{60} U could be determined from the KVV C_{60} Auger spectrum.³ Moreover, since the minimum distance between carbon atoms on different C_{60} molecules (3Å) is much larger than the covalent bond length, the interaction

should include predominant van der Waals forces, which can be described by the Lennard-Jones potential and a small short-range Coulomb interaction.²⁵ The results from the two kinds of calculations are approximately equal, ranging from 1.6 to 1.99 eV/C₆₀, and are much smaller than the bond energy between carbon atoms.

The same can also be seen from the distribution of intra- and inter-molecule electron charges (**Figures 4** and **5**). The electron density contours in **Figure 4** show an accumulation of electronic charges at each C-C bond region, indicating the formation of strong sp^{2.278} hybridised σ bonds between each pair of nearest-neighbour carbon atoms. The maximum electron density is at a position close to the spherical surface of C₆₀. This may result from the intra-spheroid inclination of σ orbitals, and rehybridising with p_z orbitals. As the distance from the carbon atoms increases, the electron density decreases rapidly. When the distance reaches 1.8au (0.952Å), the density falls to zero.

Figure 5 shows the charge density distribution of t_{1u} LUMO electrons (electrons added to the LUMO) in two-pair carbon atoms on two nearest-neighbour molecules, and illustrates the point that electron charges focus on the very small regions around carbon atoms. Because the distance between two spherical centres of adjacent molecules is about 10.02Å, when it is not yet at the mid-distance, the electron density already drops to zero. Therefore, the interaction between the valent charges (π electrons) on adjacent molecules is very weak. At room temperature, C₆₀ molecules in the FCC lattice spin at high speeds of over 10⁵ revolutions per second.

From the above, it can be seen that the interaction between fullerene C₆₀ crystal grains is very weak, and the surface energy of a C₆₀ crystal is very low, as C₆₀ molecules have a very stable closed-shell bond structure. Under mechanical compression in a sliding interface, the crystal grains would slide against each other, or be readily detached, somewhat similar to other layered solid lubricants (graphite, MoS₂, etc.). C₆₀ molecules themselves, in a sliding interface, may roll like many tiny ball bearings, leading to low friction and low wear. Owing to their low surface energy, fullerene C₆₀ crystals would adhere very little to the mating surfaces, another potential reason for lubricity. The strong bonds between the carbon atoms in its molecules make the C₆₀ molecular structure very

stable and not easily damaged, which is good for long lasting effective lubrication.

Since the C₆₀ molecules are bonded through van der Waals forces, their crystals are expected to be as soft as graphite. Experiments have shown that fullerene clusters are loosely bonded, and can be readily indented. However, the FCC phase of solid C₆₀ remains stable under hydrostatic compression to at least 20 GPa, with an atmospheric pressure isothermal bulk modulus of 18 GPa. This suggests that the C₆₀ crystal would be very hard, and capable of bearing high loads. From the valent bond structure, the σ orbital or carbon atoms is $sp^{2.278}$, and not planar sp^2 , that is, the necessary rehybridisation for a transition state to a tetrahedral bond structure (sp^3) is already well advanced in the basic state of C₆₀. It is expected that, under high pressure, $sp^{2.278}$ hybridisation may transform into sp^3 of the diamond phase. The calculated bulk modulus of C₆₀ shows that, at pressures higher than 50GPa, it could be the most incompressible solid known.^{35,37} The load-bearing capacity of the fullerene crystal enhances with the increase of its hardness. Thus, whether at high or at low loads, the C₆₀ crystal should be a good solid lubricant.

Another effect of the strong σ -bonds and stable closed-shell π -bond, is that crystal C₆₀ does not have free surface bonds, and needs no other atoms to satisfy the surface chemical bonding requirements. Its lubricity is primarily due to weak interaction, and highly stable spherical molecules. Therefore, the C₆₀ crystal should have excellent lubricity in a vacuum or humid environment, and its lubricity should not relate to the orientations of the crystals, and should be better than layered solid lubricants (graphite, MoS₂, etc.).

Tribological tests have shown the lubricity of the C₆₀ crystal. A sublimed thin film of fullerene C₆₀ exhibited low friction coefficients, ranging from about 0.18 to 0.12, when slid against a 52100 steel ball, that is, comparable to those of graphite and MoS₂ films (~0.1). Investigations with optical microscopy indicated that there was a transfer of solid C₆₀ to the surface of 52100 steel balls. This transfer may be one of the reasons for low friction and low wear.

The friction and wear characteristics of fullerene C₆₀ films are dependent on the operating conditions, i.e., load, speed, temperature, and environment. The lowest friction, as low as 0.08, and lowest wear, have been observed at elevated

temperatures (100°C), and higher speeds (24 mm/s), and in a nitrogen environment.²³ The C₆₀/C₇₀ mixtures are dispersed into liquid paraffin by solvent evaporation. The extreme pressure (EP) and antiwear behaviour of C₆₀/C₇₀ as an oil additive have been evaluated with an SRV Tester. The results showed that when C₆₀/C₇₀ is added to liquid paraffin, the EP value increases by up to 3×, the friction coefficient decreases from 0.18 to 0.11, and wear is also reduced. It has been suggested that fine dispersed C₆₀/C₇₀ powder can be used in lubricating oil as an antifriction and antiwear additive.³⁸

In addition, there have been reports about C₆₀ compounds, such as C₆₀F_n (n=6–54, integer), C₇₀F_n (n=6–64, integer)³⁹ and C₆₀H_n (n=30–70),⁴⁰ used as solid lubricants and oil additives. Of course, these are just the beginning: to understand fully the tribological properties of fullerenes, there is a lot of work to be done, especially on performance in crucial conditions, such as high vacuum, high pressure or humidity. Based on their unique structure, fullerenes have potential as a solid lubricant with very low friction, for use in a high- or super-vacuum environment (e.g. aerospace).

Not all tribological tests have shown favourable results. Blau and Haberlin⁴⁵ studied the microfrictional behaviour of fullerene (C₆₀). In their tests, the loose layers of fullerene exhibited friction coefficients (~0.6) higher than those of the other sliding couples, including steel on aluminium, where evaporated layers of fullerene gave friction coefficients (~0.14) similar to those (~0.16) of bare aluminium. The reason for the former was thought to be fullerene powder clumping together, and high-shear dense layer formation, which is hard to deform. The reason for the latter was thought to be that the evaporated layers consisted of widely dispersed, sub-micro-sized, seemingly hollow rosettes.

Bhattacharya *et al.*⁴⁶ investigated ion-beam modification of fullerene films and their frictional behaviour, in which C₆₀ films were deposited on Si₃N₄ by thermal evaporation, giving an average friction coefficient of 0.4–0.5. High-energy ion (Ag⁺) bombardment resulted in partly crystalline to amorphous C₆₀ films, which had a low friction coefficient of <0.1. They considered that C₆₀ clusters completely disintegrate upon ion impact.

These tests show that fullerene may have poor lubricity under certain conditions. For example, Blau and Haberlin conducted their sphere-on-flat sliding tests with a friction micro-

probe; load was 98.1 mN, speed 10 μm and 440 μm , thickness of loose layers in an aluminium alloy was 1–2 mm, and thinner deposits were obtained by evaporation of a fullerene-toluene solution. The rosettes on the evaporated films showed poor uniformity and compactness.

Bhattacharya *et al.* chose Si₃N₄, deposited C₆₀ films on a variety of substrates for tribological tests, the hardness of which is very high, but did not give any description of the uniformity and compactness of the films.

Blau and Haberman pointed out the tendency of fullerene powder to clump together and compress into a high-shear strength layer which is hard to deform, but did not present sufficient evidence to draw overall conclusions. We cannot firmly surmise, therefore, that fullerene C₆₀ has no lubricity: in addition to the information presented in references 23, 38, and 40, Ginzburg, *et al.*⁴⁷ found that the presence of fullerene C₆₀ improved the antifriction, antiwear and antiseize properties of lubricating oil. Xue and Zhang⁴⁸ studied the friction and wear mechanisms of C₆₀/stearic-acid Langmuir-Blodgett (LB) films, and found for C₆₀: stearic-acid = 1:4, that the friction coefficient of disordered C₆₀/stearic-acid LB films was ~0.1, and of ordered C₆₀/stearic-acid LB films was even lower, at ~0.05.

Besides being used in the form of crystal grains (molecular clusters), the question also arises as to whether fullerenes can be used in the form of a single or near-single layer of molecules similar to the distribution of surface active agents on an interface. This is a subject worthy of research. The calculated bulk modulus of a single C₆₀ molecule (843 GPa) is much higher than that of diamond (441 GPa).⁴¹ Because of the spherical structure of C₆₀ molecules and the high modulus of a single molecule, distribution in the form of a single layer of molecules would, if possible, have the greatest lubrication efficiency whether as a solid lubricant or as an oil or grease additive, under boundary lubrication. The formation of the single layer of molecules would be affected by many factors, such as load speed, temperature, and the properties of the oil, grease or of other additives, and might also involve the chemical improvement of C₆₀ itself. For given materials, oils or greases, there would be distinct load and speed parameters.

Metals

The friction coefficients between different metals and solid C₆₀ vary. The order of friction coefficients can be estimated qualitatively by comparing the Fermi energy values (E_F) of metals with the ionisation potential (IP) and electron affinity (EA) of fullerene C₆₀. If the IP or EA of C₆₀ is larger than the E_F of metals, electrons in the metals will tend to transfer to C₆₀. The calculated IP of 5.5-8.4 eV and experimental IP of 6.42-7.87 eV are slightly larger than the Fermi energy values of some metals: $E_F(\text{Al})=5.168$ eV,⁴² $E_F(\text{Cu})=5.386$ eV,⁴³ $E_F(\text{Ni})=5.712$ eV⁴³ and $E_F(\text{Ag})=6.200$ eV.⁴⁴ Thus, although there is a transfer tendency of electrons from these metals to fullerene C₆₀, it is very small. The calculated and experimental EA of 2.4-2.8 eV (not counting the very low value of 0.8 eV) are smaller than the E_F values, that is, the electrons in these metals should not transfer to C₆₀. Likewise, they cannot, because the IP of C₆₀ approximates to the E_F values of these metals, and, naturally, the lowest unoccupied molecular orbital (LUMO) level of the metals is higher than the HOMO level of C₆₀ (its energy values approximate to the IP). In other words, the transfer of electrons between the metals and fullerene C₆₀ is very difficult, except under certain special conditions.

Thus, the interaction between metals and fullerene C₆₀ is very weak, and the friction coefficients should be very low as mentioned above. According to the order of E_F values, the order of interaction should be: Al>Cu>Ni>Ag. This should also be the order of the friction coefficients between these metals and fullerene C₆₀. Of course, this point relates only to electron transfer; in reality, the factors related to friction coefficients are more complicated.

CONCLUSIONS

- (1) Because of the spherical shape of fullerene C₆₀ molecules, their weak intermolecular interaction, high chemical stability and low surface energy, the C₆₀ crystal has lubricity potential, and probable use in high vacuum, humid and other critical conditions.
- (2) At high pressure, the covalent bonds of fullerene C₆₀ would transform sp^{2.278} to sp³, resulting in formation of a hard phase. Thus, fullerene C₆₀ has a potentially high load-bearing capacity.
- (3) The interaction between metals and fullerene C₆₀ is weak, and the friction coefficients between them should also be low.

References

1. Kratschmer, W., *et al.*, *Chem. Phys. Lett.*, **170** (1990), 167.
2. Miller, J.S., *Adv. Mater.*, **3** (1991), 262.
3. Lof, R.W., *et al.*, *Phys. Rev. Lett.*, **68** (1992), 3924.
4. Weaver, J.H., *et al.*, *Phys. Rev. Lett.*, **66** (1991), 1741.
5. Heney, P.A., *et al.*, *Phys. Rev. Lett.*, **66** (1991), 2911.
6. Fisher, J.E., *et al.*, *Phys. Rev. Lett.*, **84** (1993), 14614.
7. Weltner, W., Jr., *et al.*, *Phys. Chem. Rev.*, **89** (1989), 1713.
8. Jerome, M.S., *et al.*, *Chem. Phys. Lett.*, **141** (1987), 45.
9. Newton, M.D., *et al.*, *J. Am. Chem. Soc.*, **108** (1986), 2469.
10. Hadden, R.C., *et al.*, *Pure Appl. Chem.*, **58** (1989), 137.
11. Hadden, R.C., *et al.*, *Chem. Phys. Lett.*, **131** (1986), 135.
12. Feng, J.K., *et al.*, *Hua Xue Yan Jiu Yu Yin Yong*, **3** (1991), 3132.
13. Shibuya, T.I., *et al.*, *Chem. Phys. Lett.*, **137** (1987), 13.
14. Larsson, S., *et al.*, *Chem. Phys. Lett.*, **137** (1987), 501.
15. Hadden, R.C., *et al.*, *Chem. Phys. Lett.*, **125** (1986), 459.
16. Laszlo, I., *et al.*, *Chem. Phys. Lett.*, **136** (1987), 418.
17. Satpathy, S., *Chem. Phys. Lett.*, **130** (1986), 545.
18. Dish, R.L., *et al.*, *Chem. Phys. Lett.*, **125** (1986), 465.
19. Negri, F., *et al.*, *Chem. Phys. Lett.*, **144** (1988), 31.
20. Kobayashi, K., *et al.*, *Phys. Rev. B*, **45** (1992), 13690.
21. Chen, H.S., *et al.*, *Appl. Phys. Lett.*, **59** (1991), 2956.
22. Hayment, A.D.J., *Chem. Phys. Lett.*, **122** (1985), 421.
23. Bhushan, B., *et al.*, *Trib. Trans.*, **36** (1993), 573.
24. Saito, S., *et al.*, *Phys. Rev. Lett.*, **66** (1991), 2637.
25. Lu, J.P., *et al.*, *Phys. Rev. Lett.*, **68** (1992), 1551.
26. Heiny, P.A., *et al.*, *Phys. Rev. Lett.*, **66** (1991), 2911.
27. Coulon, V. de, *Phys. Rev. B*, **45** (1992), 13671.
28. Shirley, E.L., *et al.*, *Phys. Rev. Lett.*, **71** (1993), 133.
29. Rabenau, T., *et al.*, *Phys. B*, **90** (1993), 69.
30. Takahashi, T., *et al.*, *Phys. Rev. Lett.*, **68** (1992), 1232.
31. Weaver, J.H., *et al.*, *J. Phys. Chem. Solids*, **53** (1992), 1707.
32. Schmalz, T.G., *et al.*, *Chem. Phys. Lett.*, **130** (1986), 203.
33. Hale, P.D., *J. Am. Chem. Soc.*, **108** (1986), 6087.
34. Lichtenberger, D.L., *J. Am. Chem. Soc.*, **108** (1986), 6087.
35. Schluter, M.A., *et al.*, *Mater. Sci. Eng. B*, **19** (1993), 129.
36. Nunez-Regu Eiru M., *et al.*, *Nature*, **355** (1992), 237.
37. Nunez-Regu Eiru M., *et al.*, *Europhysics Lett.*, **21** (1993), 49.
38. Yan, F.Y., *et al.*, *Mo Ca Xue Xue Bao*, **13** (1993), 59.
39. Tanigushi, M., *et al.*, *JP05*, **179** (1993), 263.
40. Shigematsu, R., *et al.*, *JP05*, **117** (1993), 174.
41. Ruoff, R.S., *et al.*, *Nature*, **350** (1991), 663.
42. Chelikowsky, J.R., *et al.*, *Solid State Commun.*, **17** (1975), 1103.
43. Tang, A.Q., *et al.*, *Jiling Da Xue Zi Ran Ke Xue Xue Bao* (1979), 109.
44. Bertom, C.M., *et al.*, *Solid State Commun.*, **23** (1977), 959.
45. Blau, P.J., *et al.*, *Thin Solid Films*, **219** (1992), 129.
46. Bhattacharya, R.S., *et al.*, *J. Mater. Res.*, **9** (1994), 1615.
47. Ginzburg, B.M., *et al.*, *Pisma Zh. Tekh. Fiz.*, **21** (1995), 38.
48. Xue, Q.J., *et al.*, *Trib. Inter.*, **28** (1995), 287.